Rigosertib potently protects against colitis-associated intestinal fibrosis and inflammation by regulating PI3K/AKT and NF-kappa B signaling pathways

Rahmani, Farzad

2020-05-15

Rahmani , F , Asgharzadeh , F , Avan , A , Barneh , F , Parizadeh , M R , Ferns , G A , Ryzhikov , M , Ahmadian , M R , Giovannetti , E , Jafari , M , Khazaei , M & Hassanian , S M 2020 , ' Rigosertib potently protects against colitis-associated intestinal fibrosis and inflammation by regulating PI3K/AKT and NF-kappa B signaling pathways ' , Life Sciences , vol. 249 , 117470 . https://doi.org/10.1016/j.lfs.2020.117470

http://hdl.handle.net/10138/327297
https://doi.org/10.1016/j.lfs.2020.117470

Rigosertib potently protects against colitis-associated intestinal fibrosis and inflammation by regulating PI3K/AKT and NF-κB signaling pathways

Farzad Rahmani, Fereshteh Asgharzadeh, Amir Avan, Farnaz Barneh, Mohammad Reza Parizadeh, Gordon A. Ferns, Mikhail Ryzhikov, Mohammad Reza Ahmadian, Elisa Giovannetti, Mohieddin Jafari, Majid Khazaei, Seyed Mahdi Hassanian

PII: S0024-3205(20)30218-6

DOI: https://doi.org/10.1016/j.lfs.2020.117470

Reference: LFS 117470

To appear in: *Life Sciences*

Received date: 9 July 2019

Revised date: 26 December 2019

Accepted date: 24 February 2020

Please cite this article as: F. Rahmani, F. Asgharzadeh, A. Avan, et al., Rigosertib potently protects against colitis-associated intestinal fibrosis and inflammation by regulating PI3K/AKT and NF-κB signaling pathways, *Life Sciences*(2020), https://doi.org/10.1016/j.lfs.2020.117470

Rigosertib potently protects against colitis-associated intestinal fibrosis and inflammation by regulating PI3K/AKT and NF-κB signaling pathways

Farzad Rahmani[1], Fereshteh Asgharzadeh[2], Amir Avan[3,4], Farnaz Barneh[5], Mohammad Reza Parizadeh[1,3], Gordon A Ferns[6], Mikhail Ryzhikov[7], Mohammad Reza Ahmadian[8], Elisa Giovannetti[9,10], Mohieddin Jafari[11], Majid Khazaei[2,3#], Seyed Mahdi Hassanian[1,3#]

1) Department of Medical Biochemistry, Faculty of Medicine, Mashhad University of Medical Sciences, Mashhad, Iran.
2) Department of Physiology, Faculty of Medicine, Mashhad University of Medical Sciences, Mashhad, Iran.
3) Metabolic syndrome Research Center, Mashhad University of Medical Sciences, Mashhad, Iran.
4) Department of Modern Sciences and Technologies, Faculty of Medicine, Mashhad University of Medical Sciences, Mashhad, Iran.
5) Faculty of Paramedical Sciences, Shahid Beheshti University of Medical Sciences, Tehran, Iran.
6) Brighton & Sussex Medical School, Division of Medical Education, Falmer, Brighton, Sussex BN1 9PH, UK.
7) Division of Pulmonary and Critical Care Medicine, Washington University, School of Medicine, Saint Louis, MO, USA.
8) Institute of Biochemistry and Molecular Biology II, Medical Faculty, Heinrich-Heine University Düsseldorf, Düsseldorf, 40223, Germany.
9) Cancer Pharmacology Lab, AIRC Start-up, University Hospital of Pisa, Pisa, Italy.
10) Department of Medical Oncology, Cancer Center Amsterdam, VU University Medical Center, Amsterdam, the Netherlands.
11) Institute for Molecular Medicine Finland (FIMM), Helsinki Institute of Life Science, University of Helsinki, Finland.

Running title: Therapeutic potency of rigosertib against colitis

 # Corresponding Authors:
Seyed Mahdi Hassanian, Ph.D.
Department of Medical Biochemistry
School of Medicine, Mashhad University of Medical Sciences
Mashhad, Iran.
Phone: (+98) 5138002375, Fax: (+98) 5138002389
E-mail: hasanianmehrm@mums.ac.ir

Majid Khazei, MD, Ph.D.
Department of Medical Physiology,
Faculty of Medicine, Mashhad University of Medical Sciences,
Mashhad, Iran.
Phone: (+98) 5138002227, Fax: (+98) 5138002389
E-mail: KhazaeiM@mums.ac.ir

Abstract

Aims: Rigosertib (RGS) is a PI3K inhibitor that exerts protective effects against tumor progression and cancer-related inflammation. This study was aimed to explore the regulatory effects of RGS on proliferative, pro-fibrotic and inflammatory factors in DSS- induced colitis mice model.

Materials and Methods: The present study integrates systems and molecular biology approaches to investigate the therapeutic potency of RGS in an experimental model of colitis specifically examining its effects on the PI3K/AKT and NF-κB signaling pathways.

Key findings: Analysis of time-resolved proteome profiling showed that PI3K-AKT inhibitors regulate expression of many proteins in all stages of inflammation, fibrogenesis and extracellular matrix remodeling. Consistent with our *in-silico* findings, RGS improved colitis disease activity as assessed by changes in body weight, degree of stool consistency, rectal bleeding and prolapse. RGS also reduced oxidative stress markers and colon histopathological score by decreasing inflammatory responses in colon tissues. Moreover, expression of pro-fibrotic and pro-inflammatory factors including *Acta 2, Col 1a1, Col 1a2, IL-1β, TNF-α, INF-γ,* and *MCP-1* were suppressed in the mice treated with RGS compared to the control group. The protective effects of RGS were mediated by inactivation of PI3K/AKT and NF-kB signaling pathways.

Significance: This study clearly demonstrates the anti-proliferative, anti-inflammatory and anti-fibrotic effects of RGS in colitis that may have implications for the treatment of colitis and colitis-associated cancer.

Keywords: Rigosertib, Colitis, Inflammation, Fibrosis, PI3K/AKT/NF-κB signaling axis

1. Introduction

Ulcerative colitis (UC) is a common form of inflammatory bowel disease (IBD) with a high global prevalence [1, 2]. UC is characterized by chronic mucosal inflammation, from rectum to proximal segments of the colon [3, 4]. Colicky abdominal pain, bloody diarrhea, fatigue, fever, and weight loss are typical clinical symptoms in UC patients [5, 6]. Most of the current treatments for colitis target inflammatory and immune responses in patients [7]. However, these therapies are often time-consuming, and are associated with adverse effects. Patients with UC are at higher risk for developing colorectal cancer [8]. The main underlying cause in the development of colitis associated cancer (CAC) is chronic colon inflammation, resulting in activation of oncogenic signaling pathways and uncontrolled cellular proliferation in the intestinal lining [9-11].

High-throughput data acquisition and systems-level approaches have provided a more holistic view of UC, but these have required computational methodologies to discover the novel targets that are amenable to drug intervention. In the light of the new findings, mucosal healing, that follows remission of inflammation, is increasingly being appreciated as being important in determining the efficacy of UC treatment, fewer remission of the disease and decreased risk of developing cancer [12]. Based on these insights, drugs that mimic the normal sequence of wound healing and resolution may serve as novel therapeutics for unresponsive and recurrent UC disease.

Rigosertib (RGS) is a novel styryl benzyl sulfone with anti-tumor properties in different types of malignancy and is currently undergoing phase III clinical trials for the treatment of myelodysplastic syndrome (MDS) [13-17]. RGS has been shown to induce G2/M cell cycle arrest and apoptosis by down-regulating the Ras/PI3K/AKT signaling axis in human cancerous cell lines [13, 17, 18]. Several studies show interplay between inflammatory and oncogenic pathways [19, 20]. However, there is no study investigating the regulatory effect of RGS on

inflammatory-associated diseases such as colitis. We have therefore, 1) integrated systems and molecular biology approaches to explore a proteome-level dataset of the normal wound healing process and compared the deregulated proteins and the genome-wide expression changes that are induced by chemicals and drugs, and based on the observation that PI3K-AKT inhibitors affect all aspects of wound healing, 2) assessed the therapeutic efficacy of RGS against colitis and 3) examined the regulatory role of PI3K/AKT/NF-κB signaling axis in the protective effect of RGS on colitis pathological symptoms. Our results demonstrate that RGS potently attenuates clinical colitis symptoms, including disease activity index, histopathological score, and inflammation. We also showed that RGS decreases two main pathological symptoms of colitis, inflammation and fibrosis, by inhibition of downstream PI3K/AKT pro-fibrotic and pro-inflammatory target genes. Our data emphasize the therapeutic potency of this novel pharmacological inhibitor in attenuating colitis-associated pathological symptoms.

2. Materials and Methods

2.1. Reagents

Dextran sulfate sodium (DSS-40kD) and RGS were purchased from Cayman Chemical Company (Ann Arbor, MI). Rabbit anti-cyclin D1, anti-phospho-p65/RelA (Ser-536), anti-PI3K (p110α), phospho-AKT (Thr-308), and secondary antibodies were purchased from Cell Signaling Technology Inc. (Beverly, MA).

2.2. Bioinformatics pipeline

Based on recently published manuscript [21], “The Human Proteome Atlas” was used to extract the shared proteins between pulmonary and colonic tissues. To identify the proteins with significant changes between different stages of wound healing, the expression value of proteins between days 3, 14, and 28 and 56 was compared. Proteins with at least +1 difference in value

indicate the genes that are up-regulated at each step, and further down regulated in the resolution phase of injury (Figure 1A). These up-regulated proteins were submitted to BinGO app in Cytoscape to enrich biological processes associated with each time-point (adjusted p-value<0.05). The Enrichr web tool (http://amp.pharm.mssm.edu/Enrichr/) was used to identify chemicals that reversed the expression of proteins in the selected biological processes. iLINCs database was used to extract the genome-wide signature induced by RGS (Signature ID: CTRS_414) (Figure 1A). The threshold for identifying significantly altered drugs was set as 0<Fold change<1 and adjusted p-value <0.05.

2.3. Animals

Eight-week-old C57BL/6 male mice were purchased from the Pasteur institute of Iran (Tehran, Iran) and maintained according to the Institutional Animal Care Guidelines. The mice were housed under a 12h light/dark cycle, at room temperature (22-25°C) with free access to food and water ad libitum. All animal experiments were performed according to the guidelines for Care and Use of Laboratory Animals approved by Mashhad University of Medical Sciences The ethic committee approval number for conducting animal experiment in this study is 951406.

2.4. Murine colitis model and experimental protocol

Experimental colitis was induced by administration of 1% (w/v) DSS in drinking water for 7 days. RGS was dissolved in sterile water and administrated intraperitoneally (i.p.). Eighteen C57BL/6 mice were randomly divided into three groups (n= 6 for each group). The control group received normal drinking water for 10 days. The DSS group received 1% DSS in drinking water for 7 days and then received only drinking water for the next 3 days. The DSS-RGS group first received DSS 1% (w/v) for 7 days, followed by RGS (200 mg/kg/day) i.p. for 7 days from day 3 until the end of the experimental period [22]. This is a well-established animal model that mimics the clinical and histological features of IBDs that can be validated for translation of mouse data

to humans [23-25]. A schematic representation of experimental procedure is presented in Fig. 1B. During the experimental period, the animals were observed daily and evaluated for disease activity index criteria (DAI) (Table 1). The loss of >20% in total body weight was use to define a humane endpoint for the study animals. At the end of experiments, blood samples were obtained and stored at -80 °C until analysis. Colonic tissues were collected and washed with cold normal saline and placed into 10% formalin or frozen in liquid nitrogen for further analysis.

2.5. Histopathological evaluation of colons

To score colorectal tissue damage, the formalin fixed colonic tissues were embedded in paraffin, sectioned and stained with haematoxylin-eosin (H&E) and Masson's trichrome. Following light microscopy analysis, stained tissues were scored according to standard histopathological criteria presented in Table 2[4]. Histological scoring was based on the severity of inflammation, crypt loss and mucosal damage. As shown in Table 2 crypt loss is scored as follows: 0, normal crypts; 1, loss of the basal one-third; 2, loss of the basal two-thirds; 3, entire crypt loss plus intact endothelium and 4, entire crypt loss with epithelium loss). Mucosal damage is scored as follows: 0: intact mucosa; 1: damage limited to mucus layer; 2: damage in sub-mucosa and 3: damage in muscular and serosa.

2.6. Measurement of malondialdehyde (MDA)

To further investigate the anti-oxidant activity of RGS, the MDA level was measured in colon tissue homogenates. briefly, 1 ml of 10% (weigh tissue/volume of saline) tissue homogenates were mixed with 2 mL of thiobarbituric acid (TBA), Trichloroacetic acid (TCA), and HCL solution in boiling water for 45 minutes and centrifuged for 10 minutes. Next, the absorbance at 535 nm was read and the MDA level was measured by $C\ (M) = A/1.65\times10^{5}$ [10].

2.7. *Measurement of total thiol groups (SH)*

To further explore the anti-oxidant role of RGS, the total thiol group was estimated by DTNB (Di-Tio nitro benzoic acid) reagent. DTNB reacts with SH groups and produces the color yellow complex. In this line, 1ml of Tris-EDTA buffer (pH = 8.6) was added to tissue homogenate and the specimen absorbance read at 412 nm against Tris-EDTA buffer alone (A1). Next, 20 µl of DTNB reagents were added to this solution and incubated at room temperature for 15 minutes. Then, the sample absorbance was measured again (A2). The absorbance of DTNB reagent was used as a blank (B). Total thiol concentration (mM) was calculated by SH (mM) = (A2-A1-B) × 1.07 / (0.05 × 13.6) [26].

2.8. Measurement of catalase (CAT) activity

The catalase (CAT) enzyme activity was detected exactly as described previously by Aebi et al. The rational of this method was based on the hydrolyzation of H_2O_2 in phosphate buffer, pH 7.0, and reducing absorbance at 240 nm. The enzyme activity can be estimated by the conversion of H_2O_2 to H_2O and O_2 in 1 min under standard situation [27, 28]. For evaluation of the CAT enzyme activity, the tissue samples were minced in small pieces and washed in twice-distilled water. Next, 1g of tissues were homogenized in 5 ml of phosphate buffer solution. The homogenized samples were centrifuged and the supernatants were employed for evaluating CAT enzyme activity.

2.9. Real-time PCR

The mRNA expression levels of inflammatory, fibrotic and proliferative genes were evaluated using specific primers obtained from Macrogene Co. (Seoul, Korea) by real-time quantitative PCR (Table 3) as described [29]. Total RNA was extracted from frozen colon tissues of mice using the RNeasy Mini kit purchased from Qiagen Inc. (Hilden, Germany). Next,

1 µg of extracted RNA was reversed transcribed into complementary cDNA by a cDNA Reverse Transcription Kit according to the manufacturer's protocol (TaKaRa Bio, Shiga, Japan) and equivalent amounts of cDNA were used for the quantitative real-time PCR reactions using the Ampliqon SYBR Green PCR Master Mix. The expression levels were normalized to the *Gapdh* as housekeeping control gene. The ΔCT was calculated by subtracting the CT value of the *Gapdh* reference gene from that of each target gene. Results were expressed as a relative fold difference between the mRNA levels of treated and untreated samples.

2.10. Western blotting

Western blotting was performed as described [20, 30]. Briefly, total protein of colon tissues were extracted using RIPA lysis buffer (25 mM Tris–HCl, pH 7.4, 150 mM NaCl, 1 mM EDTA, 0.5% Triton X100, 0.5% SDS) containing a protease and phosphatase inhibitor cocktail (Thermo Scientific Pierce, Rockford, IL). The lysate was centrifuged at 13,000g for 10 min at 4°C and the supernatant was collected. The protein concentration was measured using the Pierce BCA protein assay kit (Thermo Scientific, Rockford, IL). Protein samples (30 microgram) were subjected to electerophoresis and transferred to polyvinylidene difluoride (PVDF) membranes (Immobilon-P, Millipore, Bedford, MA). Following a blocking step (with non-fat dry milk 5% in TBS containing 0.1% tween 20), the membranes were washed with TBS three times and incubated over night with primary (1:1000) and secondary (1:3000) antibodies. The membrane was then washed with TBS three times and incubated in Super-Signal West Femto Chemiluminescent Substrate (Thermo Scientific, Rockford, IL).

2.11. Statistical analysis

One-way analysis of variance (ANOVA) and the Wilcoxon Mann–Whitney tests were used for analyzing normal and non-parametrically distributed samples, respectively. Results were presented as means ± SEM. Values obtained from three independent experiments.

Differences were considered to be statistically significant at $P < 0.05$. For statistical enrichments in the bioinformatics pipeline, False Discovery Rate (FDR) was considered significant at $P < 0.05$.

3. Results

3.1. PI3K-AKT inhibitors are effective agents against UC

Recently Schiller et al. provided *in vivo* time-resolved proteome profiling for the sequential steps in a normal wound healing process when an injury with Bleomycin was induced in the in lung epithelium [21]. They analyzed the whole tissue proteome and provided the list of protein whose expressions were altered in each step of transition from inflammatory to resolving phase of the injury. Since 1) colitis is an inflammatory condition with impaired healing and resolving process, and 2) such high throughput data could not be found in the literature for colonic tissue, it was assumed that genes commonly expressed in lung and colon epithelia would have similar dynamics in a normally resolving injury in UC. There are several publications that highlight the similarities of intestine and lung tissues in terms of function and diseases. For instance, 1) intestine and lung are both originated from foregut at embryonic stage so both have the same rigin (gut-lung axis). 2) Both tissues form the mucos-based epithelial barriers that are exposed to have similar inflammatory components such as common mucosal immune system. 3) Correlation has been observed in pulmonary involvement in patients with inflammatory bowel diseases [42-44]. To identify a drug that can reverse the expression of up-regulated proteins in each phase [12] we used “The Human Proteome Atlas” to extract the shared proteins between lung and colon tissue. As shown in Fig. 2A, similar to lung data, the extracted proteins for the colon also showed 4 clusters representing 3 distinct phases (Inflammation, fibrogenesis and remodeling) before the injury is fully resolved.

Accordingly, we observed different biological processes involved in each step (Fig. 2B). Moreover, similar to the whole dataset in the lung injury, injury is initiated by a cascade of

inflammatory responses in the colon proteome subset which is followed by the intensive protein metabolic alterations leading to fibrogenesis. Then, the healing response is initiated by metabolic alterations involving oxidation-reduction. Finally, by down-regulation of cellular respiration processes, cell adhesion-related proteins are up-regulated to fully resolve the injury. These results suggest that if the objective is to treat colitis and its consequences, we should first overcome the inflammatory/fibrogenesis phase of the disease, and then allow healing to occur; we should also pass the ECM remodeling/proliferation phase. To identify a drug that can regulate these distinct stages, we extracted the up-regulated genes in each of the 3 phases before resolution and tried to find a drug down-regulating the proteins of each phase distinctly using Enrichr web-based enrichment tool (Fig. 3). We observed that PI3K and AKT inhibitors were among the top-five chemicals that reversed the expression of up-regulated proteins in all phases of response to injury.

After selecting the shared genes that are expressed in colon and lung (n=2466 proteins), the dynamics of the protein changes were determined according to the proteomic study data. The expression status of proteins on day 56 was assumed as the reference for full resolution of injury. Thus for each phase, the proteins whose expression was higher than day 56 were selected that included the following numbers:

Day 3: n=15 proteins, Day 14: n= 180 proteins, day 28: = 73 proteins. The differentially expressed proteins in each of the mentioned days compared to day 56 were then submitted to BinGo (Fig. 2B) and EnrichR (Fig. 3A) for further analyses. To identify a drug that can reverse the expression of up-regulated proteins, we observed that PI3K-AKT inhibitors were a class of drug that affected the expression of up-regulated proteins in each of the wound healing phases implying that over-actiovation of this pathway does not allow the wound healing process to terminate. It has been shown that RGS could inhibit PI3K/AKT in solid tumors (17, 18. 45). Moreover, RGS is already under phase 3 clinical trials for CML that if approved by FDA, will have higher chance in translational repurposing for UC treatment. So we used the RGS gene

expression signature to identify genes that are mutually altered by wound healing and RGS (Fig. 3B and Supplementary file.1). These results could support the rationale that inhibition of the PI3/AKT signaling pathway may be a promising therapeutic approach in treatment of UC.

3.2. Rigosertib attenuates clinical symptoms of colitis

To validate our *in-silico* findings, we assessed the efficacy of RGS in DSS-induced colitis model in mouse (n=6 in each group). Our findings showed that all mice with experimentally-induced colitis that were not treated with RGS developed clinical features of colitis including bloody stool, diarrhea, weight loss, and a high disease activity index (DAI). RGS treatment was associated with a significant reduction in body weight loss in DSS-induced colitis mice, compared to RGS-untreated colitis group (Fig. 4A). RGS treatment attenuated the DAI in the mice with DSS-induced colitis (Fig. 4B) supporting a protective effect of this pharmacological inhibitor on features of colitis. To further investigate the therapeutic potency of RGS against colitis, the length of colons of mice were compared between the different groups. As is shown in Fig. 4C, RGS inhibited DSS-induced colon shortening in colitis mice. Furthermore, RGS improved colon weight to colon length ratio, a marker of inflammation and tissue edema (Fig. 4D). These results support the ameliorative effects of RGS on pathological symptoms in colitis.

3.3. *Rigosertib decreases colorectal tissue damage in colitis*

We studied the effect of RGS on colon tissue damage including tissue inflammation, mucosal damage and crypt loss between RGS-treated and untreated colitis mice. Our results showed that RGS had a potent protective effect on colon histological score (Fig. 5A) including inflammation score (Fig. 5B), mucosal damage (Fig. 5C) and crypt loss (Fig. 5D) in the DSS-induced colitis mice (n=6 in each group). Consistent with these findings, pathological changes were more severe in DSS group, as evidenced by increased sub-mucosal edema, morphological damage and greater inflammatory cell infiltration. However, in the RGS-treated mice, colon tissue structure was partially protected and inflammatory symptoms were decreased

(Fig. 5 E), suggesting that RGS significantly improves clinical and histological features induced by DSS in colitis.

3.4. Anti-inflammatory role of Rigosertib in colitis

Next, we studied the regulatory role of RGS in colitis-associated inflammation in mouse tissue and serum. Compared to control colitis mice, treatment of colitis mice with RGS abrogated the inhibitory effect of DSS on total thiol concentration and catalase activity, suggesting that RGS displays anti-oxidant activity in colitis (n=6 in each group) (Fig. 6A and B). Consistent with these findings, RGS reduced levels of malonyl dialdehyde (MDA) and high-sensitive C reactive protein (hs-CRP), in tissue homogenate and blood samples of DSS-induced colitis mice, respectively (Fig. 6C and D). Moreover, comparison of pro-inflammatory genes expression levels between RGS-treated and untreated colitis mice showed that RGS significantly down-regulated the expression of interleukin-1β (*IL-1β*), tumor necrosis factor alpha (*Tnf-α*), Interferon gamma (*Inf-γ*), and macrophage chemotactic protein-1 (*Mcp-1*) in colitis tissue (Fig. 6E). These results suggest that protective effects of RGS against colitis were at least partially mediated by induction of anti-oxidant and anti-inflammatory responses.

3.5. Anti-fibrotic effects of Rigosertib in colitis mice

Colonic fibrosis is characterized by excessive collagen deposition and over-expression of fibrogenic factors which is a key step in the pathogenesis of colitis [31]. To investigate the modulatory effect of RGS on collagen deposition and fibrosis, colon tissues of different groups were stained with Masson's trichrome. Histopathological staining results showed that RGS significantly decreases deposition of collagen in colon tissues of DSS-induced colitis mice, supporting the anti-fibrotic activity of this inhibitor in colitis (Fig. 7A). In agreement with these results, mRNA expression of pro-fibrotic genes including collagen type 1 alpha 1 (*Col1a1*), collagen type 1 alpha 2 (*Col1a2*), and alpha-actin-2 (*Acta 2*) were down-regulated in the colon

tissue homogenates of RGS-treated colitis mice, in comparison to the colitis control group (n=6 in each group) (Fig. 7B). These results clearly suggest that RGS has novel therapeutic properties against colitis with clinically translational potential of inhibiting key pathological colitis responses of inflammation and fibrosis in human patients.

3.6. Inhibitory effect of Rigosertib on cell proliferation in colonic tissue

It has been shown that UC patients are at higher risk for developing colorectal cancer [8]. Since RGS is an inhibitor of oncogenic Ras/PI3K/AKT signaling axis, we investigated effect of this inhibitor on colitis-associated colorectal cancer by comparing activation or expression level of proliferative regulatory pathways, including PI3K/AKT and NF-kB in colon tissue homogenates between different groups. As shown in Fig. 8A, treatment of colitis mice with RGS potently down-regulates expression of nuclear factor-kB (*RelA*), as well as AKT. Regulatory effect of RGS on cyclin D1 expression, a down-stream target gene of AKT pathway, is elicited at the post-transcriptional level (Fig. 8A and B). Consistently, RGS decreased phosphorylation and activation of AKT and NF-kB (p65/RelA) signaling pathways in colitis tissue samples (Fig. 8B and C), demonstrating protective signaling effects of RGS against colitis-induced colon cancer.

4. Discussion

In this study, we have shown for the first time that RGS significantly attenuates colitis-associated intestinal fibrosis and inflammation by modulating PI3K/AKT and NF-κB signaling pathways in a colitis mice model. Moreover, it is noteworthy that RGS potently improved disease activity index including body weight loss, diarrhea, rectal bleeding and colonic length, as well as colon histopathological score by eliciting anti-oxidative and anti-inflammatory responses in DSS-induced colitis mice model.

During colon inflammation, the oxidant/anti-oxidant balance is perturbed leading to disruption of the epithelial cell membrane which is considered as one of the initial events during

the onset of IBDs. This membrane disruption causes macrophage, neutrophil and lymphocyte infiltration into the mucosal and sub-mucosal areas which exacerbates inflammatory responses by producing inflammatory cytokines, such as TNF-α, MCP-1, IFN-γ and ILs accompanied by up-regulation of NF-kB pro-inflammatory signaling pathway [32-34]. In line with this, Peng et al. demonstrated that the expression of proinflammatory cytokines including TNF-α, IFN-γ and IL-1β were significantly increased by DSS in colitis mice model. Further studies showed the association between elevated macrophage and neutrophil infiltration, as a main resource of inflammatory cytokines, with progression of inflammation and mucosal damage. Their results indicated that inhibition of PI3K/AKT signaling suppresses leukocyte infiltration and inflammatory responses in DSS-induced colitis mice by down-regulation of inflammatory and up-regulation of anti-inflammatory cytokines [35].

Consistent with these findings, our results revealed that RGS significantly decreases inflammation and regulates oxidant/anti-oxidant balance by down-regulation of inflammatory cytokines, increasing catalase enzyme activity and regulating thiol and MDA concentrations.

Previous studies have suggested that pro-inflammatory pathways, such as NF-kB, induce tumorigenesis by up-regulating inflammatory cytokines including TNF-α and IL-1β [36, 37]. Furthermore, the PI3K/AKT signaling axis induces phosphorylation of NF-kB signaling through degradation of inhibitor of κB (IκB) [38, 39]. Based on these findings, we investigated the effect of RGS, a PI3K inhibitor, on NF-kB in DSS-induced colitis. Our results showed that RGS down-regulates cyclin D1 expression in colitis mice. Moreover, RGS suppresses NF-kB signaling pathway via down-regulation of *Nf-kb* (*RelA*) gene expression and de-phosphorylation and inactivation of p-65/RelA subunit in colitis mice.

Consistent with the regulatory effects of RGS on inflammation, we studied effect of this pharmacological inhibitor on colitis-associated fibrosis. Our results indicate that RGS treatment suppresses the expression of pro-fibrotic factors, which is in accordance with other studies, as it clearly suggests an association between inflammation and fibrosis [40, 41].

The current study explores a novel therapeutic role of RGS against colitis through inhibition of PI3K/AKT and NF-κB signaling pathways in colitis mice. The inhibitory role of RGS on proliferative signaling pathways including PI3K/AKT as well as down-stream target genes such as cyclin D1 is clinically relevant to the association between colitis as a risk factor for colon cancer [42]. The therapeutic potency of RGS against DSS-induced colon tissue degradation is mediated by suppression of inflammation and fibrosis not necessarily by regulating cell proliferation. But decrease in cell proliferation during tissue regeneration may postpone colitis treatment in patients. Further investigation should be performed to evaluate side effects of rigosertib administration in other cellular, animal and clinical studies in colitis patients. Further investigation into the mechanisms involved in the protective effects of RGS will advance our knowledge about the exact molecular mechanism of the protective signaling functions of RGS against colitis pathogenesis, colitis-associated colorectal cancer, and other pro-inflammatory and pro-fibrotic disorders for a better understanding and hence a better management of these diseases.

Acknowledgment: This study was supported by grants awarded by the Mashhad University of Medical Sciences (Grant No. 951406), and the Biotechnology Development Council of the Islamic Republic of Iran (Grant No. 960301) to S.M.H and National Institute for Medical Research Development (Grant No. 965391) to M.K.

Additional information

Competing interest: The authors declare that they have no conflicts of interest with the contents of this article.

References

1. Xiao, B., et al., *Combination therapy for ulcerative colitis: Orally targeted nanoparticles prevent mucosal damage and relieve inflammation.* Theranostics, 2016. **6**(12): p. 2250.
2. Ali, A.A., et al., *Protective effect of cardamonin against acetic acid-induced ulcerative colitis in rats.* Pharmacological Reports, 2016.
3. Dignass, A., et al., *Second European evidence-based consensus on the diagnosis and management of ulcerative colitis part 1: definitions and diagnosis.* Journal of Crohn's and Colitis, 2012. **6**(10): p. 965-990.
4. Binabaj, M.M., et al., *EW-7197 prevents ulcerative colitis-associated fibrosis and inflammation.* Journal of cellular physiology, 2019. **234**(7): p. 11654-11661.
5. Carvalho, P.B. and J. Cotter, *Mucosal Healing in Ulcerative Colitis: A Comprehensive Review.* Drugs, 2017: p. 1-15.
6. Aggarwal, A., T. Sabol, and H. Vaziri, *Update on the Use of Biologic Therapy in Ulcerative Colitis.* Current Treatment Options in Gastroenterology: p. 1-13.
7. Ilan, Y., *Oral immune therapy: targeting the systemic immune system via the gut immune system for the treatment of inflammatory bowel disease.* Clinical & translational immunology, 2016. **5**(1).
8. Lakatos, P.L. and L. Lakatos, *Risk for colorectal cancer in ulcerative colitis: changes, causes and management strategies.* World journal of gastroenterology: WJG, 2008. **14**(25): p. 3937.
9. Guo, T., et al., *Octacosanol attenuates inflammation in both RAW264.7 macrophages and a mouse model of colitis.* Journal of Agricultural and Food Chemistry, 2017.
10. Amerizadeh, F., et al., *Crocin synergistically enhances the antiproliferative activity of 5-flurouracil through Wnt/PI3K pathway in a mouse model of colitis-associated colorectal cancer.* Journal of cellular biochemistry, 2018. **119**(12): p. 10250-10261.
11. Rezaei, N., et al., *Crocin as a novel therapeutic agent against colitis.* Drug and chemical toxicology, 2019: p. 1-8.

12. Seidelin, J.B., M. Coskun, and O.H. Nielsen, *Mucosal healing in ulcerative colitis: pathophysiology and pharmacology.* Adv Clin Chem, 2013. **59**: p. 101-23.

13. Athuluri-Divakar, S.K., et al., *A small molecule RAS-mimetic disrupts RAS association with effector proteins to block signaling.* Cell, 2016. **165**(3): p. 643-655.

14. Anderson, R.T., et al., *The dual pathway inhibitor rigosertib is effective in direct patient tumor xenografts of head and neck squamous cell carcinomas.* Molecular cancer therapeutics, 2013. **12**(10): p. 1994-2005.

15. Ma, W.W., et al., *Phase I study of Rigosertib, an inhibitor of the phosphatidylinositol 3-kinase and Polo-like kinase 1 pathways, combined with gemcitabine in patients with solid tumors and pancreatic cancer.* Clinical Cancer Research, 2012. **18**(7): p. 2048-2055.

16. Roschewski, M., et al., *Phase I study of ON 01910. Na (Rigosertib), a multikinase PI3K inhibitor in relapsed/refractory B-cell malignancies.* Leukemia, 2013. **27**(9): p. 1920.

17. Bowles, D.W., et al., *Phase I study of oral rigosertib (ON 01910. Na), a dual inhibitor of the PI3K and Plk1 pathways, in adult patients with advanced solid malignancies.* Clinical Cancer Research, 2014. **20**(6): p. 1656-1665.

18. Hyoda, T., et al., *Rigosertib induces cell death of a myelodysplastic syndrome-derived cell line by DNA damage-induced G2/M arrest.* Cancer science, 2015. **106**(3): p. 287-293.

19. Soltani, A., et al., *Therapeutic potency of mTOR signaling pharmacological inhibitors in the treatment of proinflammatory diseases, current status, and perspectives.* J Cell Physiol, 2018. **233**(6): p. 4783-4790.

20. Hassanian, S.M., et al., *Inorganic polyphosphate elicits pro-inflammatory responses through activation of the mammalian target of rapamycin complexes 1 and 2 in vascular endothelial cells.* J Thromb Haemost, 2015. **13**(5): p. 860-71.

21. Schiller, H.B., et al., *Time- and compartment-resolved proteome profiling of the extracellular niche in lung injury and repair.* Mol Syst Biol, 2015. **11**(7): p. 819.

22. Knod, J.L., et al., *Murine colitis treated with multitargeted tyrosine kinase inhibitors.* Journal of Surgical Research, 2016. **200**(2): p. 501-507.

23. Miyazawa, F., et al., *Interactions between dextran sulfate and Escherichia coli ribosomes.* Biochimica et Biophysica Acta (BBA)-Nucleic Acids and Protein Synthesis, 1967. **145**(1): p. 96-104.

24. Byrne, F. and J. Viney, *Mouse models of inflammatory bowel disease.* Current opinion in drug discovery & development, 2006. **9**(2): p. 207-217.

25. Egger, B., et al., *Characterisation of acute murine dextran sodium sulphate colitis: cytokine profile and dose dependency.* Digestion, 2000. **62**(4): p. 240-248.

26. Marjaneh, R.M., et al., *Phytosomal curcumin inhibits tumor growth in colitis-associated colorectal cancer.* J Cell Physiol, 2018.

27. Aebi, H., *Catalase in vitro.* Methods Enzymol, 1984. **105**: p. 121-6.

28. Marjaneh, R.M., et al., *Phytosomal curcumin inhibits tumor growth in colitis-associated colorectal cancer.* Journal of cellular physiology, 2018.

29. Hassanian, S.M., P. Dinarvand, and A.R. Rezaie, *Adenosine regulates the proinflammatory signaling function of thrombin in endothelial cells.* J Cell Physiol, 2014. **229**(9): p. 1292-300.

30. Hassanian, S.M., et al., *Inorganic polyphosphate promotes cyclin D1 synthesis through activation of mTOR/Wnt/beta-catenin signaling in endothelial cells.* J Thromb Haemost, 2016. **14**(11): p. 2261-2273.

31. Gordon, I.O., et al., *Fibrosis in ulcerative colitis: mechanisms, features, and consequences of a neglected problem.* Inflamm Bowel Dis, 2014. **20**(11): p. 2198-206.

32. Ito, R., et al., *Interferon-gamma is causatively involved in experimental inflammatory bowel disease in mice.* Clinical & Experimental Immunology, 2006. **146**(2): p. 330-338.

33. Tian, T., Z. Wang, and J. Zhang, *Pathomechanisms of oxidative stress in inflammatory bowel disease and potential antioxidant therapies.* Oxidative medicine and cellular longevity, 2017. **2017**.

34. Yan, Y., et al., *Temporal and spatial analysis of clinical and molecular parameters in dextran sodium sulfate induced colitis.* PloS one, 2009. **4**(6): p. e6073.

35. Peng, X.-d., et al., *Inhibition of phosphoinositide 3-kinase ameliorates dextran sodium sulfate-induced colitis in mice.* Journal of Pharmacology and Experimental Therapeutics, 2010. **332**(1): p. 46-56.

36. Liu, A., et al., *Baicalein pretreatment protects against liver ischemia/reperfusion injury via inhibition of NF-κB pathway in mice.* International immunopharmacology, 2015. **24**(1): p. 72-79.

37. Luo, C. and H. Zhang, *The role of proinflammatory pathways in the pathogenesis of colitis-associated colorectal cancer.* Mediators of inflammation, 2017. **2017**.

38. Bai, D., L. Ueno, and P.K. Vogt, *Akt-mediated regulation of NFκB and the essentialness of NFκB for the oncogenicity of PI3K and Akt.* International journal of cancer, 2009. **125**(12): p. 2863-2870.

39. Ozes, O.N., et al., *NF-κB activation by tumour necrosis factor requires the Akt serine–threonine kinase.* Nature, 1999. **401**(6748): p. 82.

40. Fichtner-Feigl, S., et al., *Induction of IL-13 triggers TGF-β1-dependent tissue fibrosis in chronic 2, 4, 6-trinitrobenzene sulfonic acid colitis.* The Journal of Immunology, 2007. **178**(9): p. 5859-5870.

41. Jena, G., P.P. Trivedi, and B. Sandala, *Oxidative stress in ulcerative colitis: an old concept but a new concern.* Free radical research, 2012. **46**(11): p. 1339-1345.

42. 11972385Russell, S.J., K.W. Peng, and J.C. Bell, *Oncolytic virotherapy.* Nat Biotechnol, 2012. **30**(7): p. 658-70.

45. Prasad A., et al. *ON 01910.Na (rigosertib) inhibits PI3K/Akt pathway and activates oxidative stress signals in head and neck cancer cell lines.* Oncotarget. 2016, 29; 7(48):79388-79400.

Figure legends

Figure 1. Schematic representation of bioinformatics pipeline and experimental design of the study (A) A proteome level dataset containing time-resolved healing from lung injury was used as the initial source of high-throughput data. The Human Proteome Atlas was used to extract shared genes between colon and lung tissue. BinGO, a Cytoscape plugin was used to extract relevant biological processes involved in each step of wound healing. Enrichr and iLINCS tools and databases were used to identify and validate a drug affecting each step of normal wound healing, respectively. (B) Schematic representation of murine colitis model and experimental protocol. (C) Experimental validation steps to confirm the effect of identified drug on treatment of colitis.

Figure 2. Dynamic changes of proteins and biological processes involved in healing process of colon (A) z-score intensities of proteins that are commonly expressed in lung and colon tissue in different steps of wound healing. (B) The biological processes significantly enriched for proteins expressed in colon and altered in wound healing process. Adjusted p-value <0.05 was considered significant.

Figure 3. Drugs that reverse the expression of up-regulated proteins in each phase of normal healing from injury (A) The LINCS L1000 Down module within Enrichr web-based enrichment tool was used to identify drugs that reverse the expression of up-regulated proteins in each phase of wound healing. (B) Gene signature of Rigosertib was extracted from iLINCS database and was used to identify shared proteins in the wound healing process that are altered by RGS in each phase of wound healing.

Figure 4. Protective effects of RGS on colitis clinical symptoms (A) RGS (200 mg/kg/day;ip) decreases DSS-induced body weight loss in colitis mice (n=6 in each group). (B) Disease activity index score was compared between control group, RGS-untreated- and -treated colitis mice. (C) The inhibitory effect of RGS on DSS-induced colon shortening was measured. (D) Colon weight to colon length ratio as a marker of inflammation was compared between control group, RGS-treated and –untreated colitis mice. Each experiment was performed in triplicate.*p<0.05; **p<0.01

Figure 5. RGS attenuates colon tissue damage in colitis mice. (A) Colon damage histological score is compared between different groups (n=6 in each group). (B) RGS abrogates DSS-induced inflammation in colitis mice. (C) The same as panel B except that mucosal damage score was measured between groups. (D) The same as panel B except that the protective effect of RGS on DSS-induced crypt loss was investigated. (E) Hematoxylin and eosin (H&E)-stained sections of colons from indicated groups of mice showing representative histopathological damage and crypt loss induced by DSS on day 10. Black arrows indicate colon crypts. Each experiment was performed in triplicate. *p<0.05; ***p<0.001.

Figure 6. Anti-oxidant and anti-inflammatory responses of RGS in colitis. Colitis mice were treated with or without RGS and (A) Total thiol concentration, (B) catalase activity, and (C) MDA level were measured in colon tissue homogenates (n=6 in each group). (D) Serum concentration of high-sensitive C reactive protein (hs-CRP) was compared in the serum samples between groups. (E) RGS significantly decreased expression level of pro-inflammatory genes in colitis mice, compared to untreated colitis group. Each experiment was performed in triplicate. *p<0.05; **p<0.01; ***p<0.001.

Figure 7. RGS attenuates fibrosis in colitis. (A) Histopathological staining with Masson's trichrome showed decreased collagen deposition (blue stained, black arrows) in the RGS-treated group compared to DSS group (n=6 in each group). (B) Expression levels of pro-fibrotic genes are suppressed in RGS-treated colitis group. Each experiment was performed in triplicate. **p<0.01.

Figure 8. RGS suppresses proliferative and inflammatory signaling pathways in colitis.

(A) RGS significantly down-regulates mRNA levels of *Akt*, *Nf-kb* (*RelA*), and *Cyclin D1*, compared to un-treated colitis group (n=6 in each group). (B) Colon tissues were homogenized and expression level of PI3K and cyclin D1 as well as phosphorylation levels of AKT and p-65 were evaluated between different groups. (C) Quantitative analysis of PI3K and cyclin D1 protein expression and AKT and p-65 phosphorylation between groups. Each experiment was performed in triplicate.

Table 1. Disease activity index (DAI) was scored at the time of procedure.

Disease activity index				
Score	**Rectal bleeding**	**Stool consistency**	**Rectal prolapse**	**Lose weight**
0	None	Normal	None	<5%
1	Red	Soft	Sign of prolapse	5-10%
2	Dark red	Very soft	Clear prolapse	10-15%
3	Gross bleeding	Diarrhea	Extensive prolapse	>15%

Table 2. Colorectal tissue damage was scored according to histopathological criteria.

score	**0**	**1**	**2**	**3**	**4**
Inflammation	None	Mild	moderate	Severe	
Mucosal damage	None	Mucus layer	Submucosa	Muscular and serosa	
Crypt loss	None	1/3	2/3	100%+Intact epithelium	100% with epithelium lose
Pathological change range	none	1-25%	26-50%	51-75%	76-100%

Table 3. qPCR primer sequences

Gene	Source	Primer	sequence
Gapdh	Mouse	Forward	CAACGACCCCTTCATTGACC
		Reverse	CTTCCCATTCTCGGCCTTGA
Col 1a1	Mouse	Forward	AATGGTGAGACGTGGAAACC
		Reverse	GACAGTCCAGTTCTTCATTGCA
Col 1a2	Mouse	Forward	GTTCTCAGGGTAGCCAAGGT
		Reverse	CCTTCAAAACCAAAGTCATAGCC
Acta-2	Mouse	Forward	CCCAGACATCAGGGAGTAATGG
		Reverse	TCTATCGGATACTTCAGCGTCA
Cyclin D1	Mouse	Forward	GCGTACCCTGACACCAATCTC
		Reverse	ACTTGAAGTAAGATACGGAGGGC
Akt-1	Mouse	Forward	TGAACGACGTAGCCATTGTG
		Reverse	GTGCCATCGTTCTTGAGGAG
Nf-kb (RelA)	Mouse	Forward	CCAAGGACATGACTGCTCAA
		Reverse	AGACGCTGCCTCTGAAGTTT
Tnf-α	Mouse	Forward	AGGCTGTCGCTACATCACTG
		Reverse	CTCTCAATGACCCGTAGGGC
Il-1β	Mouse	Forward	GACTTCACCATGGAATCCGT
		Reverse	TGCTCATTCACGAAAAGGGA
Ifn-γ	Mouse	Forward	TGGCTGTTTCTGGCTGTTAC
		Reverse	CTCTTTTCTTCCACATCTATGCC
Mcp-1	Mouse	Forward	GTGAAGTTGACCCGTAAATCTGA
		Reverse	ACTAGTTCACTGTCACACTGGT

Conflict of interest: The authors declare that they have no conflicts of interest with the contents of this article.

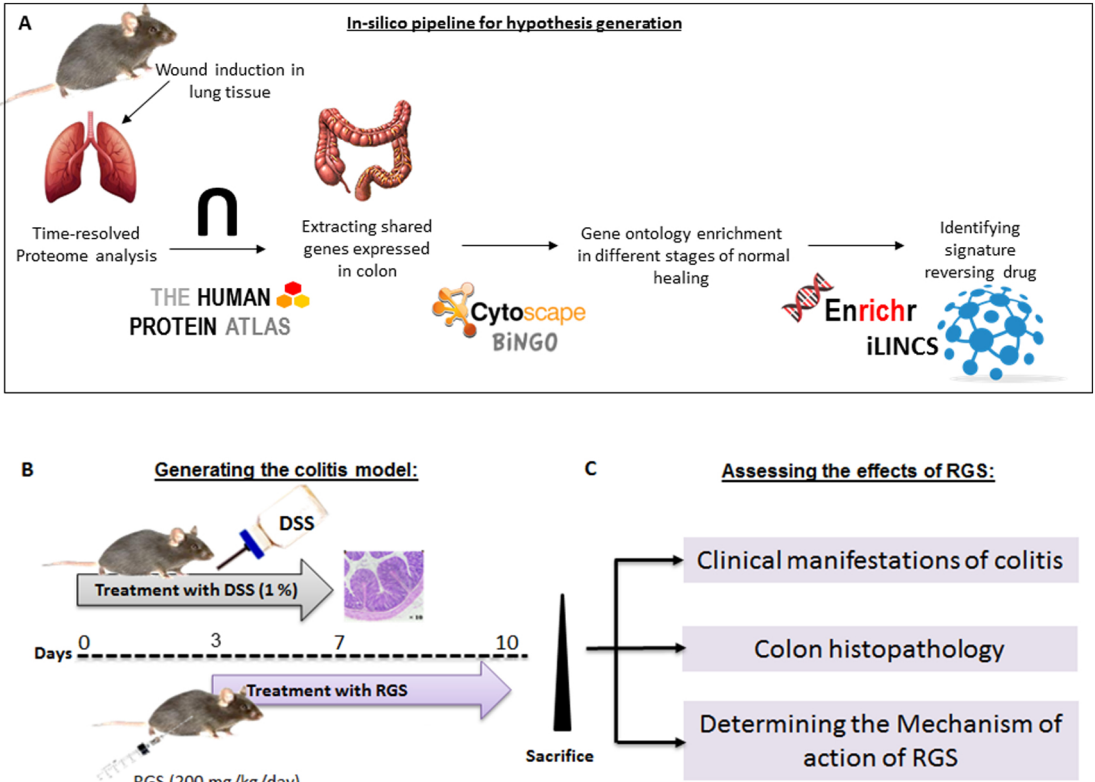
A
In-silico pipeline for hypothesis generation
Wound induction in lung tissue
Time-resolved Proteome analysis
THE HUMAN PROTEIN ATLAS
Extracting shared genes expressed in colon
Cytoscape
BiNGO
Gene ontology enrichment in different stages of normal healing
Identifying signature reversing drug
Enrichr
iLINCS
B
Generating the colitis model:
DSS
Treatment with DSS (1 %)
Days 0 3 7 10
Treatment with RGS
RGS (200 mg/kg/day)
Sacrifice
C
Assessing the effects of RGS:
Clinical manifestations of colitis
Colon histopathology
Determining the Mechanism of action of RGS

Figure 1

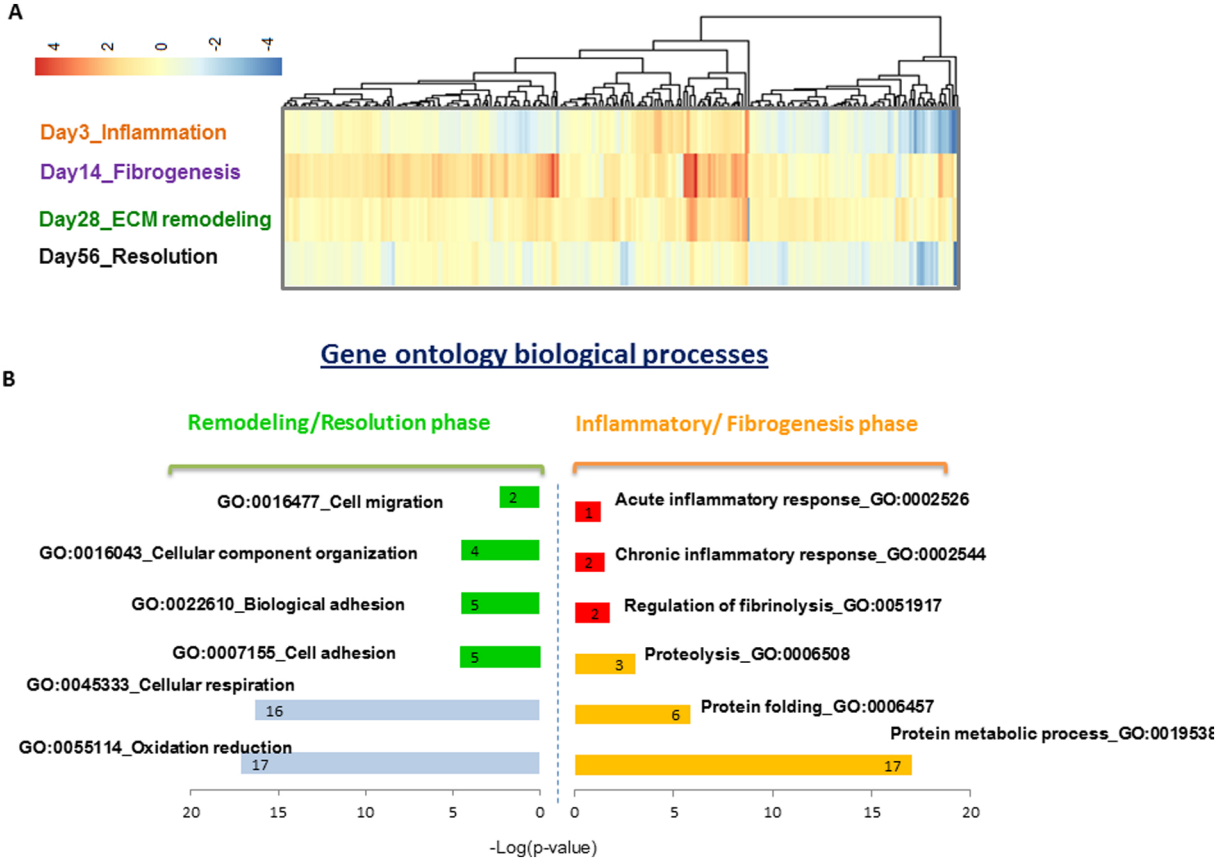
A
4
2
0
-2
-4
Day3_Inflammation
Day14_Fibrogenesis
Day28_ECM remodeling
Day56_Resolution
Gene ontology biological processes
B
Remodeling/Resolution phase
Inflammatory/ Fibrogenesis phase
GO:0016477_Cell migration
2
GO:0016043_Cellular component organization
4
GO:0022610_Biological adhesion
5
GO:0007155_Cell adhesion
5
GO:0045333_Cellular respiration
16
GO:0055114_Oxidation reduction
17
Acute inflammatory response_GO:0002526
1
Chronic inflammatory response_GO:0002544
2
Regulation of fibrinolysis_GO:0051917
2
Proteolysis_GO:0006508
3
Protein folding_GO:0006457
6
Protein metabolic process_GO:0019538
17
20
15
10
5
0
0
5
10
15
20
-Log(p-value)

Figure 2

A

Time point	Chemical name	q-value	Mechanism of Action
Inflammatory phase	A443654 (0.37μM)	3.43E-07	**AKT inhibitor**
	3H-GSK-1059615 (1.11μM)	9.91E-04	**AKT inhibitor**
	3H-PHA-793887 (0.37 μM)	1.04E-03	CDK2 inhibitor
	radicicol (1.11μM)	9.91E-04	
	afatinib (10μM)	9.91E-04	
Fibrogenesis phase	QL-X-138 (10μM)	2.56E-03	BTK-MNK inhibitor
	GSK-2126458 (3.33μM)	2.56E-03	**PI3K inhibitor**
	QL-XII-47 (1.11μM)	3.64E-03	BTK inhibitor
	ponatinib (1.11μM)	2.19E-02	Bcr-Abl inhibitor
	AZ20 (1.11μM)	3.54E-02	ATM-ATR inhibition
ECM remodeling phase	QL-XII-47-1.11μM	1.85E-04	BTK inhibitor
	QL-X-138 (3.33 μM)	2.36E-04	BTK inhibitor
	OSI-027 (1.11 μM)	5.23E-04	mTOR inhibitor
	GDC-0068 (10 μM)	2.36E-04	**AKT inhibitor**
	torin-1 (0.37μM)	2.36E-04	

B

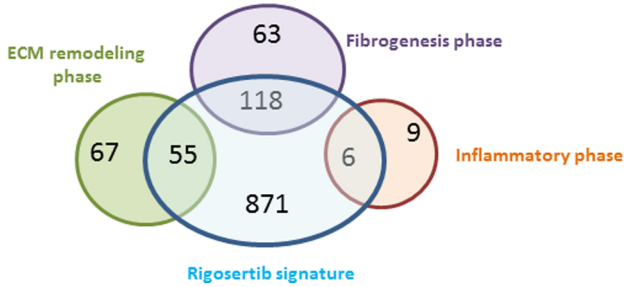

Figure 3

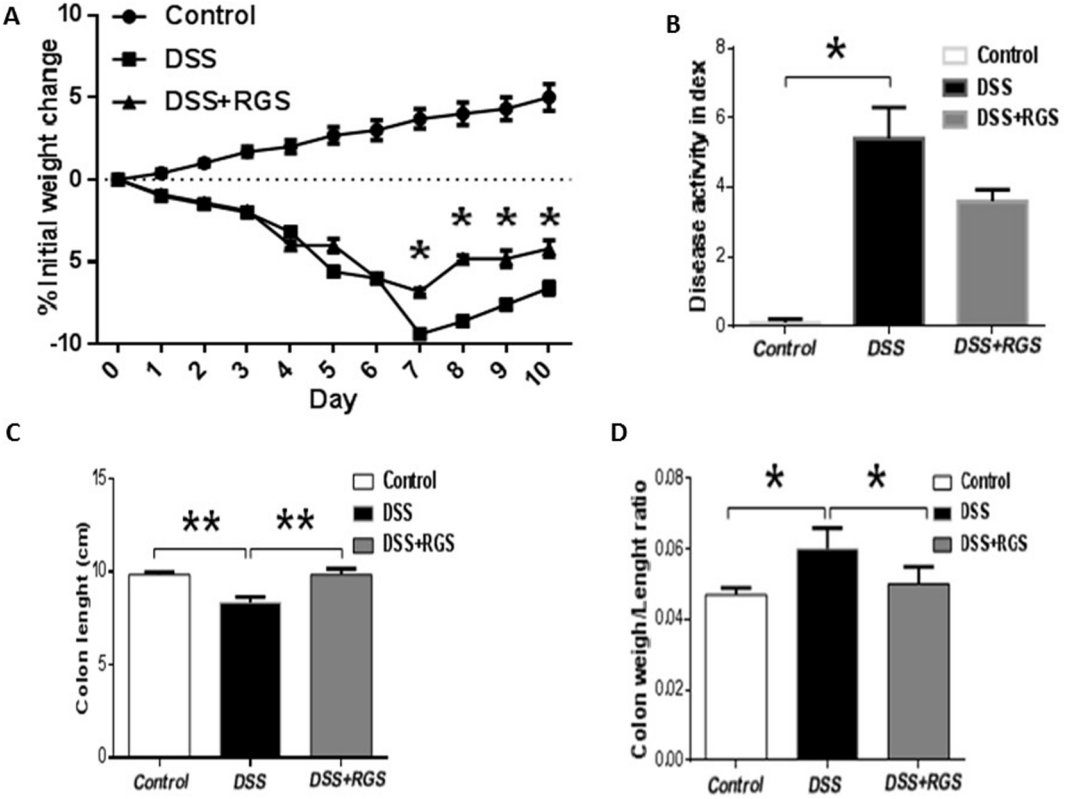
A
Control
DSS
DSS+RGS
% Initial weight change
Day
B
Disease activity in dex
Control
DSS
DSS+RGS
C
Colon lenght (cm)
Control
DSS
DSS+RGS
D
Colon weigh/Lenght ratio
Control
DSS
DSS+RGS

Figure 4

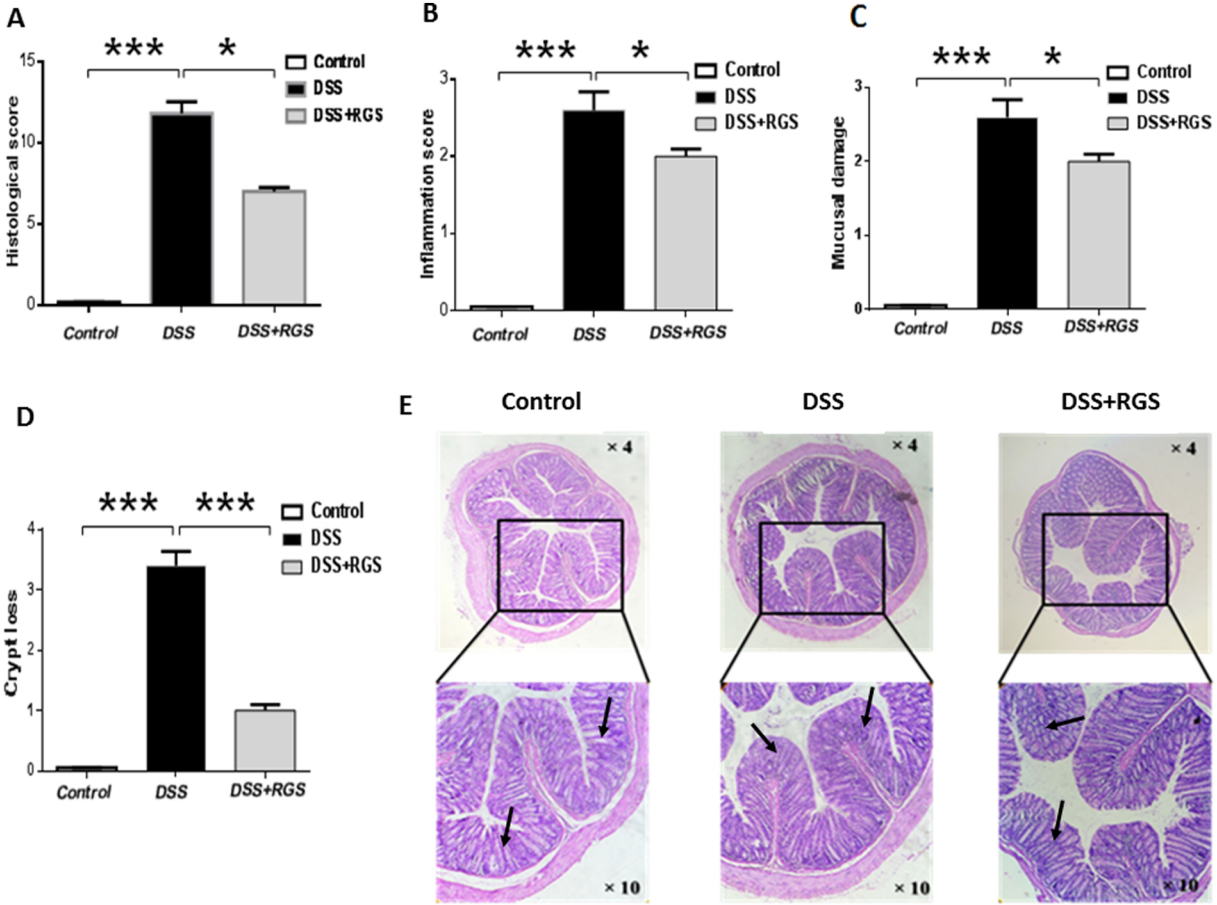
A
***
*
Control
DSS
DSS+RGS
Histological score
15
10
5
0
Control
DSS
DSS+RGS
B
***
*
Control
DSS
DSS+RGS
Inflammation score
3
2
1
0
Control
DSS
DSS+RGS
C
***
*
Control
DSS
DSS+RGS
Mucusal damage
3
2
1
0
Control
DSS
DSS+RGS
D
***
***
Control
DSS
DSS+RGS
Crypt loss
4
3
2
1
0
Control
DSS
DSS+RGS
E
Control
DSS
DSS+RGS
× 4
× 10

Figure 5

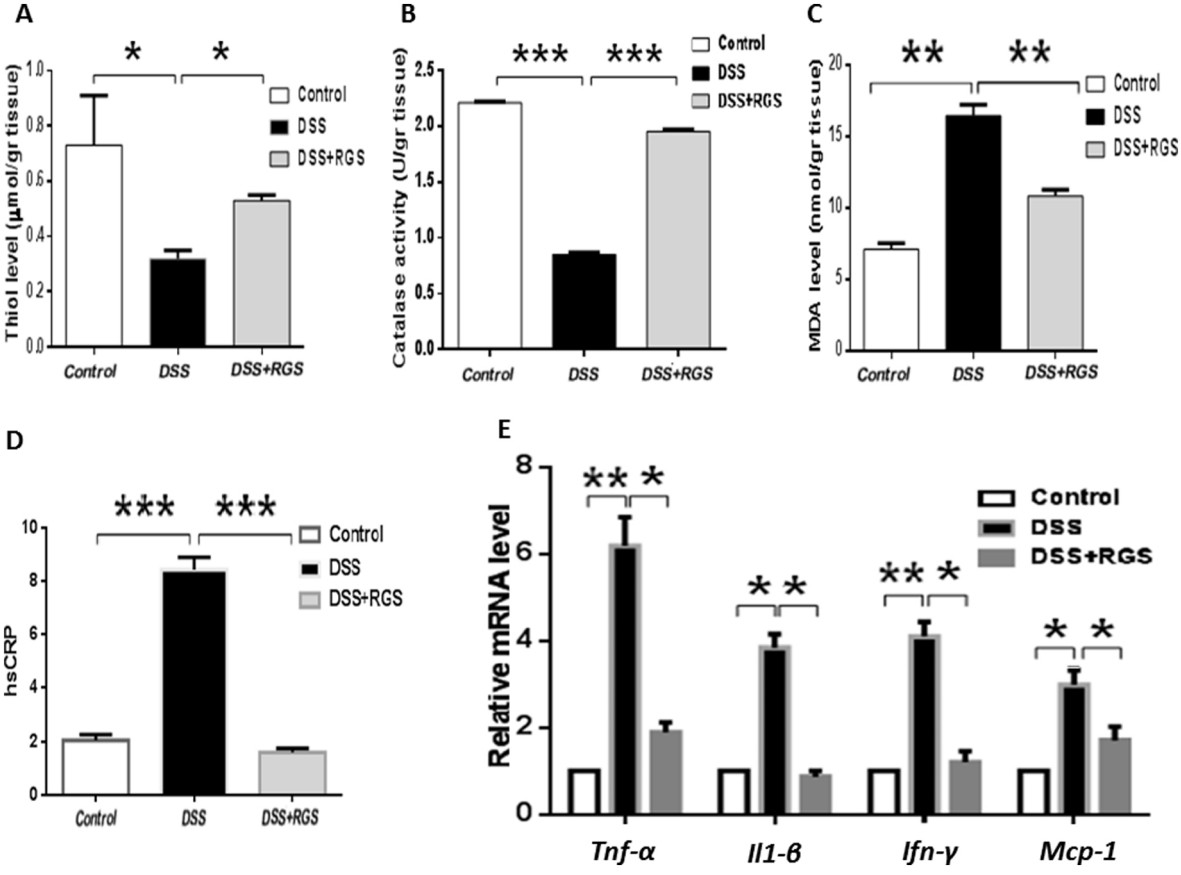
A
Thiol level (µmol/gr tissue)
Control
DSS
DSS+RGS
B
Catalase activity (U/gr tissue)
C
MDA level (nmol/gr tissue)
D
hsCRP
E
Relative mRNA level
Tnf-α
Il1-β
Ifn-γ
Mcp-1

Figure 6

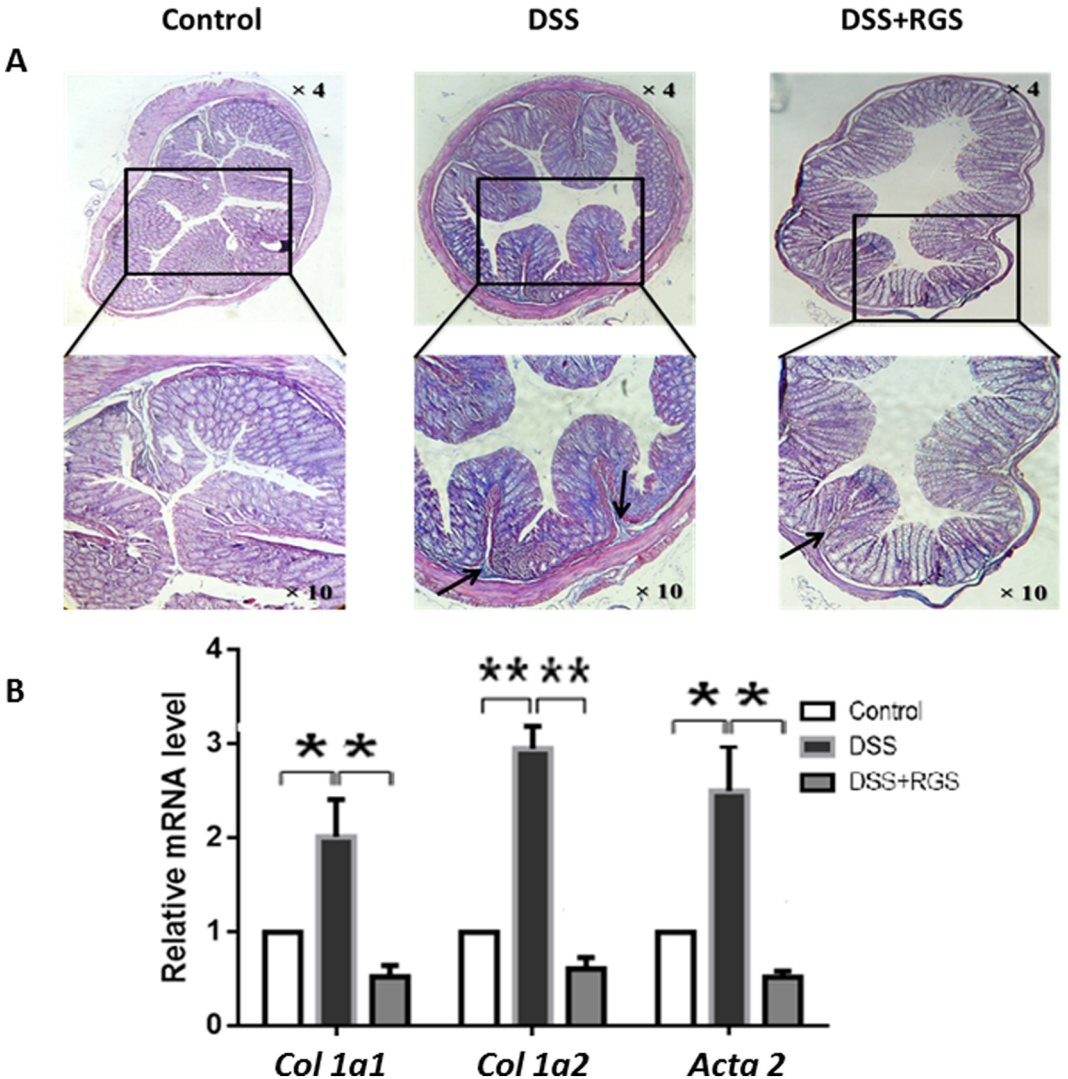
Control
DSS
DSS+RGS
A
× 4
× 10
B
Relative mRNA level
Control
DSS
DSS+RGS
Col 1a1
Col 1a2
Acta 2

Figure 7

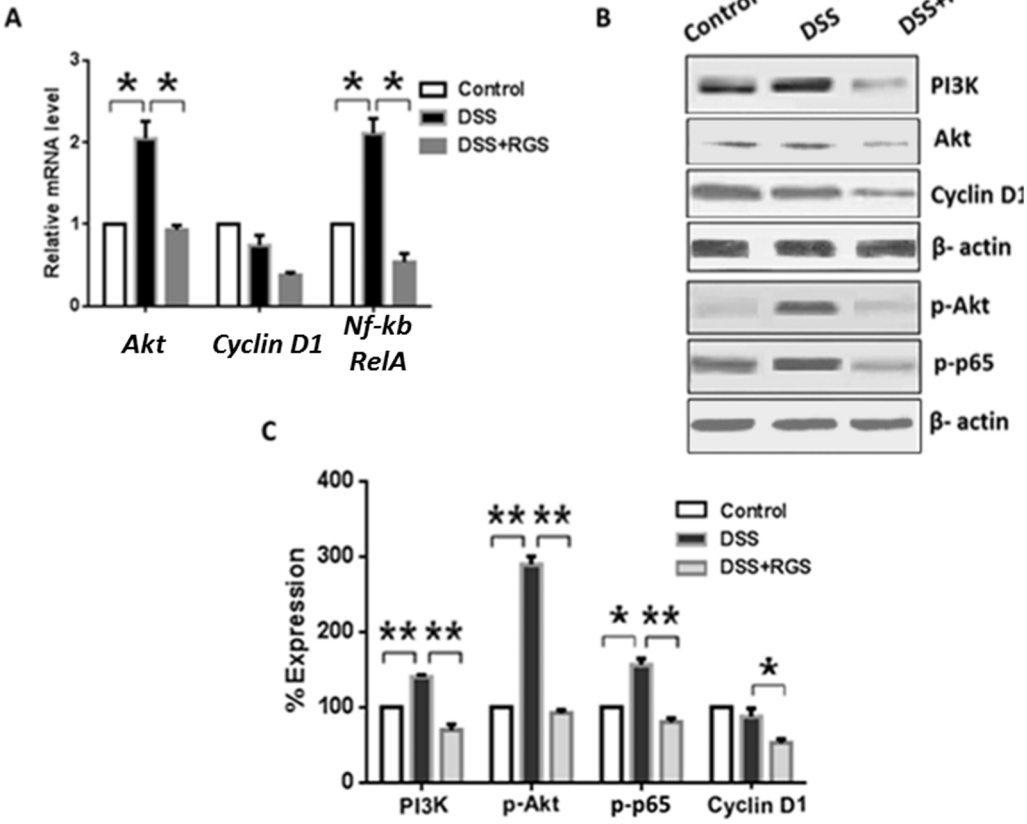
A
Relative mRNA level
3
2
1
0
Control
DSS
DSS+RGS
Akt
Cyclin D1
Nf-kb RelA
B
Control
DSS
DSS+RGS
PI3K
Akt
Cyclin D1
β- actin
p-Akt
p-p65
β- actin
C
% Expression
400
300
200
100
0
Control
DSS
DSS+RGS
PI3K
p-Akt
p-p65
Cyclin D1

Figure 8